In situ beam trajectory tilt measurement based on single cavity beam position monitor

Jian Chen, Shanshan Cao, Luyang Yu, Longwei Lai, Renxian Yuan, and Fangzhou Chen
Shanghai Advanced Rearch Institute, Chinese Academy of Sciences, Shanghai 201204, China

Yongbin Leng*
University of Science and Technology of China, Hefei 230026, Anhui, China

(Received 27 July 2023; accepted 25 September 2023; published 10 October 2023)

In recent decades, high-gain free-electron lasers (FELs) based on linear accelerators has been successfully developed around the world. Advanced beam diagnostics and feedback technology is one of the key factors to further improve the performance of facilities. Both beam position deviation and trajectory tilt can weaken the interaction between the electron beam and photon beam in the undulator, and seriously affect the FEL radiation performance. Existing measurement methods are not sufficient to achieve accurate measurement of beam trajectory tilt between compact undulator segments. Based on the working principle of beam-cavity, this paper proposes a method based on the measurement results of a single cavity BPM signal, which can simultaneously achieve real-time and *in situ* measurement of beam position and trajectory tilt, thus opening up a new way to improve the efficiency of FEL radiation. The feasibility of the scheme has been verified with the CBPM system in the Shanghai Soft X-ray FEL facility (SXFEL). The preliminary beam experiment results show that the resolution of beam trajectory tilt is better than 13.3 μrad with a bunch charge of 100 pC.

DOI: 10.1103/PhysRevAccelBeams.26.102802

I. INTRODUCTION

High-gain free-electron lasers (FELs) based on linear accelerators are recognized as fourth-generation light sources. Compared with third-generation synchrotron radiation facilities, they have the characteristics of high brightness, full coherence, ultrasmall spatial resolution, and ultrafast temporal resolution [1,2]. The most stringent performance requirements for the BPM system in terms of single-shot resolution are motivated by the achievement of optimal electron-photon beam overlap along the undulator sections and the provision of highest pointing stability of the x-ray beam toward the experimental end stations. The beam transverse position deviation can be measured by a high-resolution beam position monitor, such as a cavity BPM, and then can be corrected in combination with a correction magnet [3–5]. However, from the longitudinal perspective of the electron beam, due to the finite and discrete distribution of BPMs in the accelerator, when restoring the ideal beam radiation orbit using BPM data, only the beam position at the discrete BPM locations is recovered. The longitudinal beam exit direction (trajectory tilt) at the BPM locations is uncertain, as shown in Fig. 1. This is one of the main reasons for the drastic deterioration of FEL radiation when restoring the radiation orbit based on BPM recorded values during operation.

Therefore, if real-time measurement of beam trajectory tilt can be performed and combined with the beam position, the full information extraction of the motion state and motion trend of the beam in space can be realized, which

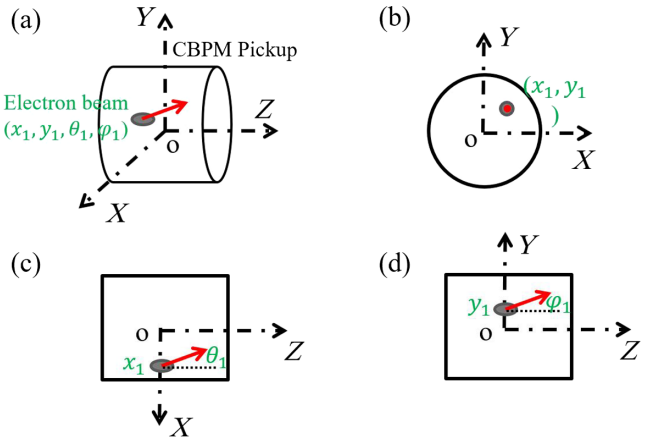

FIG. 1. Diagram of the 4-dimension parameters for beam trajectory with tilt.

*lengyb@ustc.edu.cn

will be beneficial for accelerator physicists and operation engineers to analyze the physical processes of the electron beam and reduce the uncertainty parameters of the bunch during operation.

Generally, the trajectory tilt can be calculated from two position data, such as using two adjacent beam position monitors [6], and the angle resolution is dependent on the position resolution and the distance between the two BPMs. The advantage of this method is that the measurement principle is simple and has high angle resolution. But on the other hand, it is necessary to build a drift section for two BPMs, which occupies a large space, so it is not suitable for use in space-constrained areas such as undulator sections. In addition, measuring the parameter of beam trajectory tilt requires a higher cost to equip two sets of BPM systems.

Cavity BPM (CBPM), which adopts a resonant cavity structure and uses the characteristic modes excited by the electron beam to measure beam parameters, has the advantage of high resolution and is widely used in FEL facilities [7–13]. The wake field of different modes carries different bunch information, the amplitude and phase of the signals of different modes can be extracted through the signal processing method to obtain the characteristic parameters of the source bunch.

II. DETECTION PRINCIPLE OF CAVITY BPMs

A short, relativistic electron bunch, passing near the center of the cavity pickup, will excite electromagnetic fields of a narrow bandwidth (compare to other monitors like stripline or button BPMs). The amplitudes and frequencies of the excited eigenmodes in the cavity depend on its particular configuration, and different modes signal carry different characteristic parameters of the electron beam.

For a typical cylindrical pill-box cavity BPM, the electrical fields induced by a beam passing close to the center of a cavity can be derived from the D'Alembert equation [14]. Its solutions lead to Bessel functions J_m of the order $m = 0$ and 1 as the first two eigenmodes, TM_{010} and TM_{110} modes. The amplitude and phase of these modes carry characteristic parameters of the source bunch, such as bunch charge, bunch length, beam arrival time, beam position and trajectory tilt, etc. The axial electric field component of the TM_{110} mode in cylindrical coordinates can be expressed as [15–18]

$$E_c(\rho,\phi,z) = E_0 J_1\left(\frac{\chi_{11}\rho}{r}\right)\cos(\phi)e^{-i\omega_{110}t}. \quad (1)$$

And the TM_{010} mode can be expressed by

$$E_c(\rho,z) = E_0 J_0\left(\frac{\chi_{01}\rho}{r}\right)e^{-i\omega_{010}t}, \quad (2)$$

where E_0 is the amplitude of the electric field and J_m is the Bessel function of the first kind of order m, χ_{11} is 3.832, χ_{01} is 2.405, r is the cavity radius, ω_{010} and ω_{110} are the resonant angular frequencies of the TM_{010} and TM_{110} modes, and (ρ,ϕ,z) is the position in cylindrical coordinates.

Due to the finite conductivity of metal, each resonant mode of the cavity has an energy loss. When the cavity stores an energy U for a resonant mode with angular frequencies of ω and it loses a power P, the loaded quality factor Q_L is defined as

$$Q_L = \frac{\omega U}{P}. \quad (3)$$

And the relationship of Q_L, Q_0, and Q_{ext} can be defined as

$$\frac{1}{Q_L} = \frac{1}{Q_0} + \frac{1}{Q_{\text{ext}}}. \quad (4)$$

The Q_0 is the internal quality factor which mainly caused by cavity material, geometry and surface roughness. Q_{ext} is the external quality factor which caused by external port of the cavity.

The output power of the cavity is described by the normalized impedance R/Q, which represents the interaction between the beam and the cavity. It is not related to the cavity material but related to the cavity structure and size. When the beam passes the cavity with the orbit s, and the electric field of the excited modes of the cavity is E, the normalized shunt impedance can be expressed by

$$\frac{R}{Q} = \frac{|\int Eds|^2}{\omega U}. \quad (5)$$

Assuming that the electron beam has a Gaussian distribution, the bunch length is σ_z, the bunch charge is q, the output power can be written as

$$P_{\text{out}} = \frac{\omega U}{Q_{\text{ext}}} = \frac{q^2\omega^2}{4Q_{\text{ext}}}\left(\frac{R}{Q}\right)e^{-\frac{\omega^2\sigma_z^2}{c^2}}. \quad (6)$$

If the impedance of the port is Z and consider the simple harmonic oscillation of the signal with time, so the output signal of the cavity port can be written as:

$$V_{\text{port}}(t) = \frac{q\omega}{2}\sqrt{\frac{Z}{Q_{\text{ext}}}\left(\frac{R}{Q}\right)}e^{-\frac{\omega^2\sigma_z^2}{2c^2}}e^{-\frac{t}{\tau}}\sin(\omega t+\phi). \quad (7)$$

τ is the decay time of the cavity resonant mode. Considering that the bunch length of the FEL facility is in the order of hundreds of femtoseconds, the bunch length term is close to 1. According to Eqs. (1) and (2), the R/Q of TM_{110} and TM_{010} modes can be calculated, respectively, so the output voltage of these two main resonant modes of the cavity can be calculated, expressed as

$$V_{110} = A_1 q J_1\left(\frac{\chi_{11}\rho}{r}\right)e^{-\frac{t}{\tau_{110}}}\sin(\omega_{110}t+\phi_1), \quad (8)$$

$$V_{010} = A_0 q J_0\left(\frac{\chi_{01}\rho}{r}\right)e^{-\frac{t}{\tau_{010}}}\sin(\omega_{010}t+\phi_0), \quad (9)$$

where the A_0 and A_1 represent the parameters for the TM_{010} and TM_{110} modes, respectively. Once the cavity structure is determined, these values become constants. ϕ_0 and ϕ_1 represent the initial phase of the signals for the TM_{010} and TM_{110} modes, respectively. Therefore, near the center of the cavity. Using the Bessel function approximation,

$$J_m(\rho) \sim \frac{1}{m!}\left(\frac{\rho}{2}\right)^m. \tag{10}$$

The excited voltage of the TM_{110} mode is zero when the beam is at the cavity center without tilt and is proportional to the beam offset and beam charge. The excited voltage of the TM_{010} mode is independent of the beam position but is proportional to the beam charge. When the beam pass through from both sides of the position cavity center, the phase difference of the TM_{110} signal remains fixed. But in typical applications, the phase of TM_{110} with respect to the reference resonator is defined as 0 and 180° for both polarizations of the dipole mode. Therefore, a monopole TM_{010} mode cavity is also employed to eliminate the variation of bunch charge and provide a reference phase. In addition, when the beam trajectory has different tilts, the difference will also be reflected in the phase of the TM_{110} mode relative to the TM_{010} mode, so it can be used to measure the beam trajectory tilt. The detailed analysis will be introduced in Sec. III.

III. THEORETICAL ANALYSIS OF BEAM TILT MEASUREMENT

According to the detection principle of cavity BPM, the signal coupled out by the position cavity (TM_{110} mode) is mainly composed of the following parts: the signal of beam position offset (V_{pos}), the signal excited by the beam trajectory tilt in the cavity (V_{tilt}), the signal excited by the bunch with an angle of α ($V_{\mathrm{bunch\text{-}angle}}$), the crosstalk signal between the position cavities and reference cavity to the position cavity ($V_{\mathrm{crosstalk}}$), and the last is the noise floor of the system (V_{noise}). Thus, the influence and properties of each component of the signal can be analyzed one by one to explore the possibility of beam trajectory tilt measurement.

The first term represents the signal excited when the beam pass through the cavity on a trajectory parallel to the z-axis, which can be expressed by Eq. (8), and the noise floor that determines the resolution limit of the system. The analysis of these two parts is often mentioned in the performance evaluation of the high-resolution CBPM system for beam position measurement and will not be repeated here [19].

A. Beam trajectory tilt of θ

For a bunch of charge q, with a finite length σ_z pass through the cavity. Let us first consider a simple case where the bunch passes through the center of the cavity but on a trajectory with an angle of θ relative to the z-axis. In this case, the response of a cavity to such a bunch can be easily analyzed by equating the cavity as being comprised of many thin cavities stacked along the z-axis. Then the bunch can be considered to pass parallel to the z-axis with a certain offset in each thin cavity [20], as shown in Fig. 2.

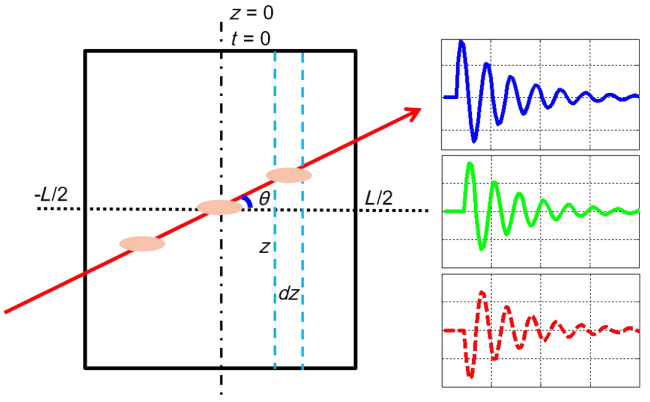

FIG. 2. Diagram of the bunch passing through the center of the cavity with a trajectory tilt of θ.

For the TM_{110} mode, when a bunch passes through the cavity parallel to the z-axis with an offset of x, the Eq. (7) can be expressed as Eq. (11) for easier understanding.

$$V_{\mathrm{port}}(t) = \frac{q\omega}{2}\sqrt{\frac{Z}{Q_{\mathrm{ext}}}\left[\frac{R}{Q}\right]_0}\frac{x}{x_0}e^{-\frac{\omega^2\sigma_z^2}{2c^2}}e^{-\frac{t}{\tau}}\sin(\omega t+\phi). \tag{11}$$

Here, $[\frac{R}{Q}]_0$ represents the shunt impedance when the bunch deviates from the electrical center of the cavity by x_0. Thus, if the bunch length is assumed to be stable and the cavity parameters are also fixed, the constant terms can be separated

$$A = \frac{q\omega}{2x_0}\sqrt{\frac{Z}{Q_{\mathrm{ext}}}\left[\frac{R}{Q}\right]_0}e^{-\frac{\omega^2\sigma_z^2}{2c^2}}. \tag{12}$$

Then the output voltage can be simply expressed as

$$V_{\mathrm{port}}(t) = Axe^{-\frac{t}{\tau}}\sin(\omega t+\phi). \tag{13}$$

Therefore, as mentioned above, for the bunch passing through the center of the cavity with a trajectory tilt of θ, and the cavity with length L is divided into several thin cavities with a length of dz, as illustrate in Fig. 2, the bunch passes straight through each thin cavity with an offset of x

$$x = z\tan\theta. \tag{14}$$

Then the signal from the thin cavity can be expressed as

$$dv = Az\tan\theta e^{-\frac{t}{\tau}}\sin(\omega t)\frac{\mathrm{d}z}{L}. \tag{15}$$

The total signal can be obtained by summing the signals from each thin cavity through integration from $-L/2$ to $L/2$. In addition, the transit time need to be considered. Setting the cavity center as time zero, then the integrated signal can be expressed as

$$V_\theta = A\int_{-L/2}^{L/2} z\,\tan\theta\,\exp\left[-\frac{t+z/c\,\cos\theta}{\tau}\right]\sin\left[\omega\left(t+\frac{z}{c\,\cos\theta}\right)\right]\frac{\mathrm{d}z}{L}$$
$$= \frac{A\tan\theta}{L}e^{-t/\tau}\int_{-L/2}^{L/2} z\,\exp\left[-\frac{z}{\tau c\cos\theta}\right]\left[\sin\omega t\cos\left(\frac{\omega z}{c\cos\theta}\right)+\cos(\omega t)\sin\left(\frac{\omega z}{c\cos\theta}\right)\right]\mathrm{d}z. \quad (16)$$

When the resonant period of the cavity signal is much smaller than the decay time, that is $2\pi \ll \tau$, the integral of $e^{-\frac{z}{\tau c\cos\theta}}$ from $-L/2$ to $L/2$ is approximately equal to 1, and $z\,\sin(\omega t)\cdot\cos(\frac{\omega z}{c\cos\theta})$ is an odd function, the integral from $-L/2$ to $L/2$ is zero. Thus, the Eq. (16) reduces to

$$V_\theta \approx \frac{A\tan\theta}{L}e^{-t/\tau}\int_{-L/2}^{L/2} z\left[\cos(\omega t)\sin\left(\frac{\omega z}{c\cos\theta}\right)\right]\mathrm{d}z$$
$$= \frac{A\tan\theta}{L}e^{-t/\tau}\cos(\omega t)\left[\frac{2c^2\cos^2\theta}{\omega^2}\sin\frac{\omega L}{2c\cos\theta} - \frac{Lc\cos\theta}{\omega}\cos\frac{\omega L}{2c\cos\theta}\right]. \quad (17)$$

Comparing the forms of Eqs. (13) and (17), it can be noticed that the output signal induced by a bunch passing through the cavity center with trajectory tilt of θ, is $\pi/2$ out of phase with the case that the bunch is parallel to the z-axis with an offset of x. Therefore, this signal cannot be canceled by the beam offset in the horizontal and vertical directions, which also has a significant impact on the precise measurement of the beam position by cavity BPMs.

In addition, the numerical simulation based on Eq. (17) shows that the output voltage V_θ is approximately proportional to the square of the cavity length L (the resonant frequency of the cavity is set to be 5.775 GHz), as shown in Fig. 3.

Furthermore, let us consider a more common case where the bunch still passes through the cavity with a trajectory tilt of θ, but not through the center of the cavity, and intercepts the z-axis at m, as shown in Fig. 4.

In this case, the method of dividing the cavity into several thin cavities for integration is also adopted, and it can be expressed as

$$V_\theta = A\int_{-L/2}^{L/2}(z-m)\tan\theta\,\exp\left[-\frac{t+z/c\,\cos\theta}{\tau}\right]\sin\left[\omega\left(t+\frac{z}{c\,\cos\theta}\right)\right]\frac{\mathrm{d}z}{L}$$
$$= \frac{A\tan\theta}{L}e^{-t/\tau}\cos(\omega t)\left[\frac{2c^2\cos^2\theta}{\omega^2}\sin\frac{\omega L}{2c\cos\theta} - \frac{Lc\cos\theta}{\omega}\cos\frac{\omega L}{2c\cos\theta}\right]$$
$$- \frac{Am\tan\theta}{L}e^{-t/\tau}\cdot\frac{2c\cos\theta}{\omega}\cdot\sin\left(\frac{\omega L}{2c\cos\theta}\right)\sin(\omega t). \quad (18)$$

From the reduced results of Eq. (18), it can be seen that the first term is exactly the same as Eq. (16), representing the contribution due to the trajectory tilt. And the phase of the second term is the same as the phase when the bunch passing through the cavity parallel to the z-axis, which is equivalent to the contribution of a fixed offset parallel to the z-axis. It is worth noting that in this case, the phase of the signal output by the cavity is no longer $\pi/2$ from the position offset signal, but has a phase difference of β. According to Eq. (18), it can be described as

$$A\cos(\omega t) + B\sin(\omega t) = \sqrt{A^2+B^2}, \quad (19)$$

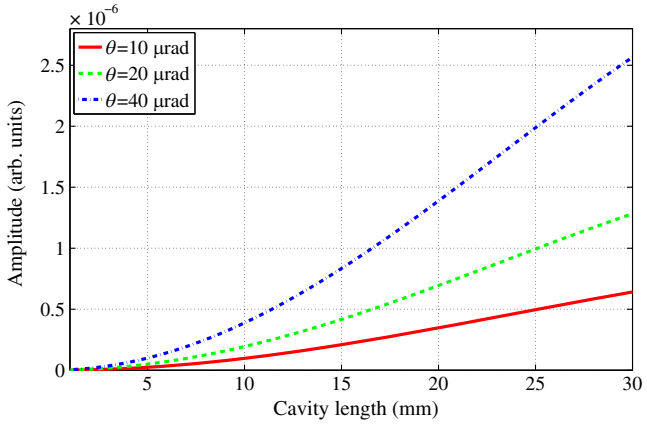

FIG. 3. The approximate relationship between V_θ and cavity length based on numerical simulation.

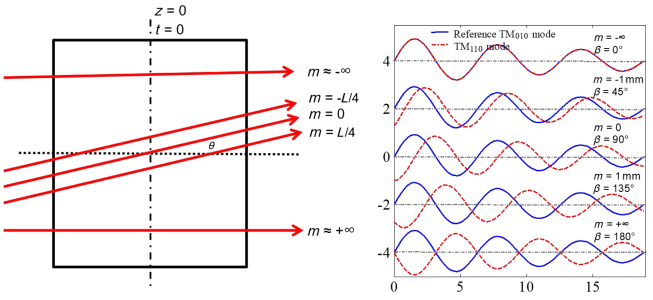

FIG. 4. The diagram of the bunch through the cavity with a trajectory tilt of θ but not through the center of the cavity.

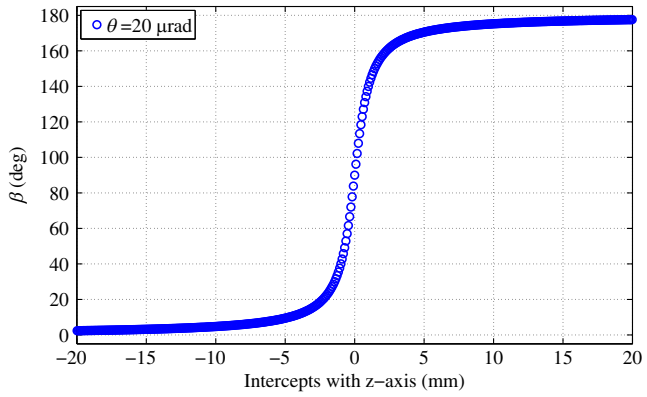

FIG. 5. Phase change of cavity output signal when the bunch passes through the cavity with different intercepts m.

$$\cos\beta = \frac{B}{\sqrt{A^2+B^2}}. \tag{20}$$

Based on the numerical simulation, it can be obtained the phase change and amplitude of output signal when the bunch passes through the cavity with different intercepts m, as shown in Figs. 5 and 6.

B. Bunch with an angle of α

As shown in Fig. 7, considering a finite bunch length, the centroid of the bunch passes through the cavity along the z-axis, only the bunch with an angle of α.

Similar to the previously analyzed method, the response of the cavity to such a bunch can be easily analyzed by equating the bunch as a series of particles distributed along the z-axis, with each particle having charge of dq and an offset of $z\tan(\alpha)$ when passing through the cavity. Assuming that the bunch is Gaussian distributed along the z-axis, then dq can be defined as

$$d_q = \frac{q}{\sqrt{2\pi}\sigma_z} e^{-\frac{z^2}{2\sigma_z^2}dz}. \tag{21}$$

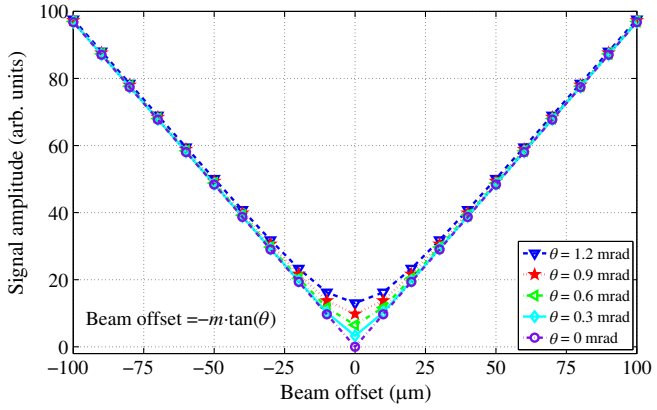

FIG. 6. Amplitude of cavity output signal when the bunch passes through the cavity with different intercepts m.

Combining with Eq. (11), we can let the constant term be A_α, expressed as

$$A_\alpha = \frac{q\omega}{2x_0}\sqrt{\frac{Z}{Q_{\text{ext}}}\left[\frac{R}{Q}\right]_0} e^{-\frac{\omega^2\sigma_z^2}{2c^2}}. \tag{22}$$

The total signal can be obtained by integrating the charge over the entire space, with the cavity center set as time zero. The integrated signal can be expressed as:

$$\begin{aligned} V_\alpha &= A_\alpha \frac{\tan\alpha}{\sqrt{2\pi}\sigma_z}\int_{-\infty}^{\infty} z\exp\left[-\frac{z^2}{2\sigma_z^2}\right]\exp\left[-\frac{t-\frac{z}{c}}{\tau}\right] \\ &\quad\times\sin\left[\omega\left(t-\frac{z}{c}\right)\right]\mathrm{d}z \\ &\approx A_\alpha\frac{\omega\sigma_z^2\tan\alpha}{c}e^{-\frac{t}{\tau}}\cos(\omega t). \end{aligned} \tag{23}$$

From the Eq. (23), it can be noticed that the output signal induced by a bunch with an angle passing through the cavity along the z-axis is also out of phase by $\pi/2$ compared to the case where the bunch is parallel to the z-axis with an offset of x. Furthermore, based on numerical calculations, it can be concluded that the output signal amplitude of the bunch with an angle is nearly 10 orders of magnitude smaller compared to the beam trajectory tilt of the same size. Therefore, its effect can be approximately ignored.

C. Crosstalk between cavities

Regarding crosstalk between cavities, the TM_{110} mode of the CBPM position cavity is taken as the object of analysis. This mainly includes crosstalk between the reference cavity and the position cavity, as well as crosstalk between the X and Y direction dipole modes of the position cavity. As analyzed in Chapter 6 of the Ref. [21], the effect of crosstalk between reference cavity and position cavity can be expressed as

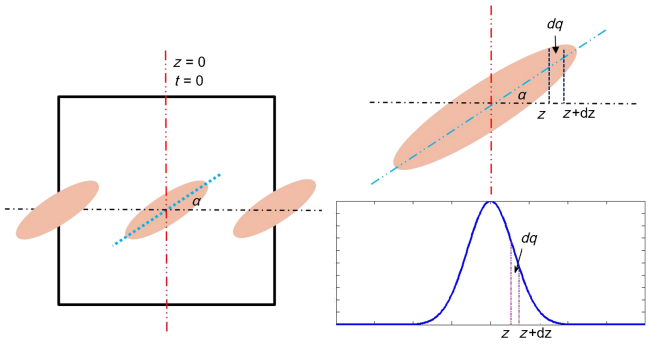

FIG. 7. The diagram of the bunch passes through the cavity along the z-axis and the bunch with an angle of α.

$$\mathrm{Pos}_{\mathrm{mea}} = \frac{(1+\Delta m)A_{\mathrm{pos}} + (1+\Delta m)A_{\mathrm{ref}} \cdot C}{(1+\Delta m)A_{\mathrm{ref}}} \cdot k_{\mathrm{pos}} = \frac{A_{\mathrm{pos}}}{A_{\mathrm{ref}}} \cdot k_{\mathrm{pos}} + C \cdot k_{\mathrm{pos}}. \quad (24)$$

where the subscripts ref and pos represent the reference cavity and position cavity, respectively. A_{pos} and A_{ref} represent the signal magnitude for the corresponding cavities. Δm is the variation of the cavity signal due to the jitter of the bunch charge, and C is the crosstalk between the reference cavity and position cavity.

The effect of crosstalk between X and Y direction dipole modes of the position cavity can be expressed as

$$\mathrm{Pos}Y_{\mathrm{mea}} = \frac{(1+\Delta m)A_y}{(1+\Delta m)A_{\mathrm{ref}}} k_y + \frac{(1+\Delta m)(A_x+\Delta A_x)}{(1+\Delta m)A_{\mathrm{ref}}} k_x C_{x-y} = \frac{A_y}{A_{\mathrm{ref}}} k_y + \frac{A_x}{A_{\mathrm{ref}}} k_x C_{x-y} + \frac{\Delta A_x}{A_{\mathrm{ref}}} k_x C_{x-y}. \quad (25)$$

Δm represents the variation of the cavity signal due to the jitter of the bunch charge, and C_{x-y} and ΔA_x are the crosstalk factor from the horizontal dipole mode to the vertical dipole mode and the beam position jitter of the X-direction, respectively. k_x and k_y represent the calibration factor for the corresponding cavities.

Since the phases of the position cavity and the reference cavity are in the same phase, according to Eq. (11), it can be considered as sin term, and the effects of the crosstalk between the cavities finally reflected in the measurement accuracy and resolution of the system, so it does not affect the measurement of the beam trajectory tilt.

D. Summary

Based on the above analysis, the effects on the composition of the cavity BPM output signal are determined. The total signal coupled out by the position cavity TM_{110} mode can be expressed as

$$V_{\mathrm{mea}} = V_{\mathrm{pos}} + \mathrm{i}V_{\mathrm{orbit\text{-}tilt}} + \mathrm{i}V_{\mathrm{bunch\text{-}angle}} + V_{\mathrm{crosstalk}} + V_{\mathrm{noise}}. \quad (26)$$

It can be seen that the third item has a negligible impact, while the fourth and fifth items affect the system resolution. The first and second items are the contributions of beam offset and trajectory tilt, which are the focus of our measurement.

From the results shown in Figs. 5 and 6, it is evident that if the relative phase and amplitude of the output signal can be combined and analyzed using the method of orthogonal decomposition in the digital domain, it is expected to demodulate the beam trajectory tilt, and the equivalent beam offset can also be demodulated simultaneously. This will enable monitoring of not only the transverse two-dimensional beam position (X and Y) but also the longitudinal two-dimensional movement trend of the beam at the pickup using single cavity BPM. Moreover, it will also improve the performance of the cavity BPM system, eliminating the need for deliberate deeccentricity work to achieve precise measurement of the beam position by the cavity BPM.

IV. BEAM EXPERIMENT AND DATA ANALYSIS

A. Beam experiment setup

In 2020, a C-band cavity BPM system was designed and developed for the Shanghai High repetition rate x-ray Free Electron Laser and Extreme Light facility (SHINE). This system is capable of achieving a beam position resolution

TABLE I. Main parameters of the C-band CBPM system.

CBPM pickup	X dipole mode	Y dipole mode	Reference cavity
Resonant frequency (MHz)	5775	5770	5769
Loaded Q	3458	3796	3746
Cavity length (mm)	8.5	8.5	5
Sensitivity (V/nC)	1.29/mm	1.29/mm	9.27
Crosstalk (dB)	−44 (X to Y)	−47 (Y to X)	−75 (position to reference)
rf front-end		Value	
LO frequency (MHz)		5712	
IF frequency (MHz)	63	58	57
DBPM processor		Value	
Maximum sampling rate (MSPS Max)		1000	
Analog bandwidth (GHz)		1.2	
ADC bits		16	

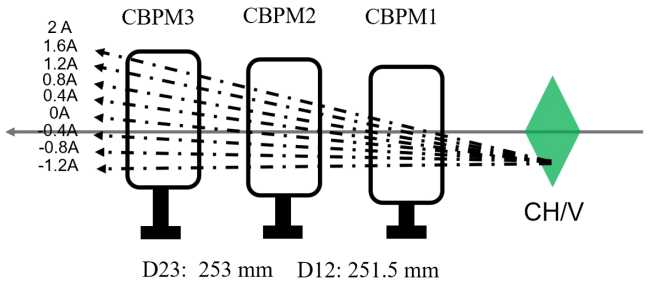

FIG. 8. The diagram of the beam test bench and geometrical distribution of the cavity pickups.

better than 200 nm at the bunch charge of 100 pC, making it suitable for verification experiments of the beam trajectory tilt measurement. The main parameters of this C-band CBPM system are summarized in Table I [18,22–27].

Based on the analysis results presented earlier, an experiment program was designed, and a beam test bench with three adjacent C-band CBPM pickups was built in the drift section at the end of the linear accelerator of the Shanghai soft X-ray Free Electron Laser facility (SXFEL) [28,29]. Figure 8 shows the diagram of the beam test bench and the geometrical distribution of the cavity pickups. The photo of the test bench is shown in Fig. 9.

Each cavity BPM pickup is installed on a two-dimensional motion platform, which allows for calibration of the position conversion factor of the CBPM system and evaluation of the relative phase change of the cavity pickup at different beam position offsets during the experiment. The corrector H/V located approximately 5 m upstream of the cavity pickups in the Fig. 8 can be used to change the trajectory tilt of the beam during the experiment. The absolute value of the change in the beam trajectory tilt can be calculated by using the measured beam position and the geometric spacing of the CBPM1 and CBPM3, which completes the calibration of the angle conversion factor of the measurement system. Additionally, combining the two measurement results of trajectory tilt for data correlation

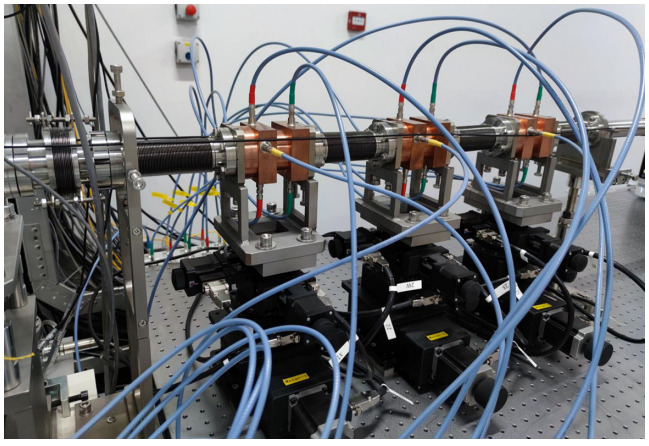

FIG. 9. The photo of the beam test bench.

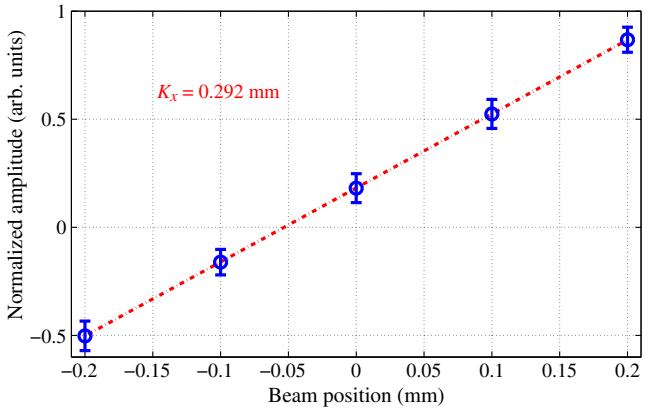

FIG. 10. The position conversion factor of the CBPM system.

analysis can also evaluate the resolution of the beam trajectory tilt measurement.

During the experiment, the bunch charge under operating conditions was measured to be 98 pC using the integrating current transformer (ICT). Taking into account the beam jitter of SXFEL, which is about 100 μm peak to peak, and the adjustment of the trajectory tilt, the dynamic range of the CBPM system was set to ±300 μm. The two-dimensional motion platform was set in steps of 100 μm from −200 to 200 μm, so the position conversion factor of the cavity BPM system was obtained as shown in Fig. 10.

To simulate the beam with a trajectory tilt passing through the cavity pickup at different eccentric positions (with different intercepts from the z-axis), the current of the corrector was adjusted so that the beam passed through the cavity pickup with a trajectory tilt. The CBPM2 was then constantly moved by the two-dimensional motion platform, and the change of the relative phase was evaluated. The results are shown in Fig. 11, which are consistent with the theoretical results shown in Fig. 5.

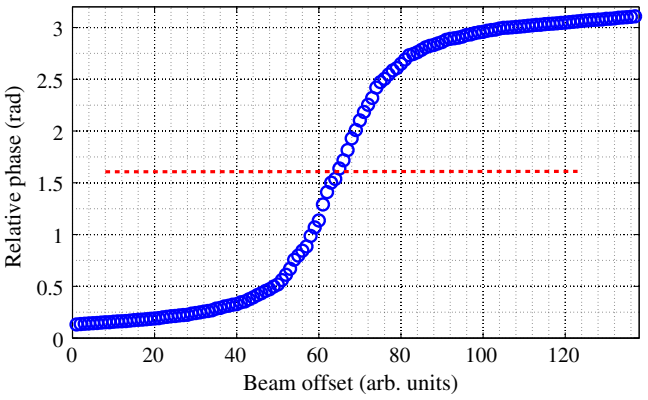

FIG. 11. The change of the relative phase when the beam with a trajectory tilt pass through the cavity pickup at different beam offsets (the red dotted line means the relative phase change of $\pi/2$).

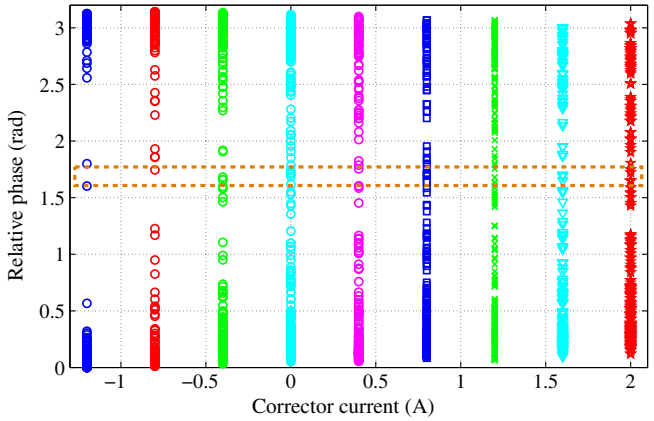

FIG. 12. The relative phase distribution at different trajectory tilts. The red dotted box represents the relative phase change of the signal, which is approximately close to $\pi/2$. This corresponds to the data samples where the beam with the trajectory tilt just passing through the center of the cavity, as used in Fig. 13.

B. Measurement methods and data analysis

Two methods are used for the measurement of the beam trajectory tilt, which are compared and checked against each other.

1. Center-finding method

The first method involves constructing the condition in which the beam can pass through the center of the cavity. Based on the analysis in Sec. III, when the beam passes through the center of the cavity with a trajectory tilt, the phase of the position cavity relative to the reference cavity changes by $\pi/2$, and the normalized amplitude is mainly determined by the angle of the beam trajectory. In the experiments, beams with different trajectory tilt were constructed by adjusting the corrector currents upstream of the cavity pickups from -1.2 to 2 A with the step of 0.4 A, as shown in Fig. 8. Under the adjusted angle of each beam trajectory, the position of CBPM2 is moved through the two-dimensional motion platform under the pickup, so that the beam can passes close to the center of the cavity. Due to the jitter of the beam, the accumulated data when the beam is close to the center can be used to judge and extract the data passing through the center of the cavity in combination with the relative phase change. The phase distribution of the measured data under different beam trajectory tilts is shown in Fig. 12, and within the dotted line a box is formed where the phase change of $\pi/2$ is visible, indicating that the beam has just passed through the center of the cavity.

Then, the amplitude under different beam trajectory tilts are calculated using the fast Fourier transform (FFT) in combination with the data samples within the accepted phase range (approximately set within 10% of $\pi/2$, as shown the red dotted box in Fig. 12). Additionally, the absolute value of the trajectory tilt is calculated using the position measurements of CBPM1 and CBPM3, and the

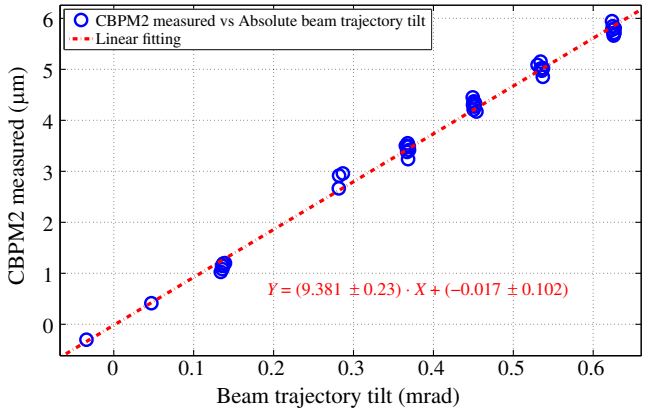

FIG. 13. The relationship between the CBPM2 measured and the absolute trajectory tilt converted by the CBPM1 and CBPM3.

linear relationship between them is shown in Fig. 13. The unit of the vertical axis has been converted to micrometers (μm) by applying a position conversion factor to the detected signal amplitude. The measurement sensitivity for the beam trajectory tilt is found to be 106 μrad/μm.

The advantage of this method is that the principle is simple, and the part coupled with the beam eccentric is removed directly in the physical mode, so the measured results are all excited by the beam trajectory tilt. However, the disadvantages are also evident. First, it is necessary to move the two-dimensional platform during the measurement to allow the beam to pass through the center of the cavity, making *in situ* measurement impossible. Second, a large amount of data must be accumulated to find samples with a phase change of $\pi/2$ for processing, and it will be very difficult to obtain data samples that pass through the center of the cavity when the beam trajectory tilt is very small. Nevertheless, this method can be used to verify the accuracy of the second method.

2. In situ demodulation method

Therefore, exploring how to analyze and separate the beam offsets and trajectory tilt under normal conditions is a worthwhile problem. According to the analysis in Sec. III A, when the beam has trajectory tilt but does not

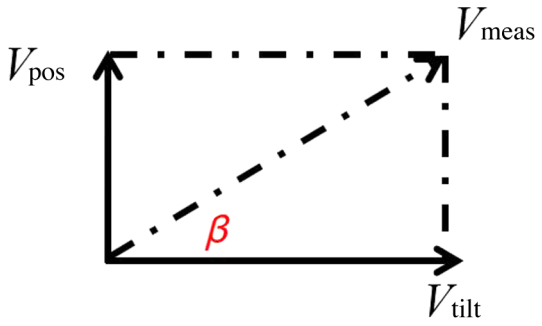

FIG. 14. The diagram of the quadrature demodulation of cavity BPM measured.

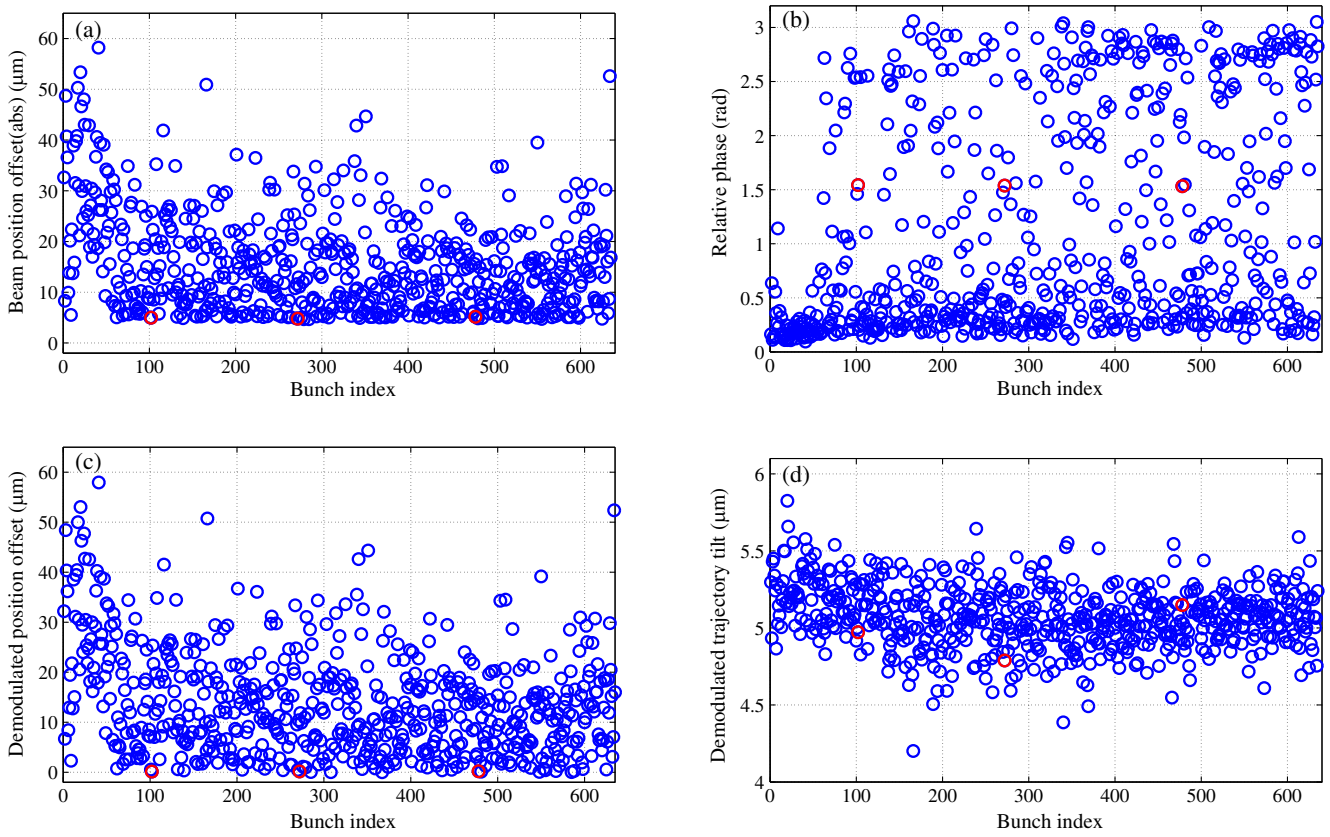

FIG. 15. (a) Beam position directly measured by CBPM2 (including beam jitter). (b) Relative phase directly measured by CBPM2. (c) Beam position demodulated from CBPM2 measurements. (d) Contribution of beam trajectory tilt demodulated from CBPM2 measurements.

pass through the cavity center, the coupled output signal can be decomposed into an equivalent position offset (sin) parallel to the z-axis and the beam with trajectory tilt and pass through the center of the cavity (cos). Since they have a fixed phase difference of $\pi/2$, the coupling signal can be separated by quadrature demodulation in the digital domain, enabling *in situ* measurement of beam position and trajectory tilt. The relationship between them can be simply shown in Fig. 14, where the measured coupling signal V_{meas}, the relative phase is β. Using the quadrature demodulation, the V_{pos} and the V_{tilt} can be expressed as

$$V_{\mathrm{pos}} = V_{\mathrm{meas}} \cdot \sin(\beta), \tag{27}$$

$$V_{\mathrm{tilt}} = V_{\mathrm{meas}} \cdot \cos(\beta). \tag{28}$$

For the analysis of experimental data, 635 sets of data with a corrector current of 1.6 A were demodulated to extract beam trajectory tilt for verification, as shown in Fig. 15. The red samples in the figure have a relative phase change of $\pi/2$, which are considered to be the comparison samples with trajectory tilt and passing near the center of the cavity.

From the comparison results in Fig. 15, it can be seen that the beam position calculated directly by the measured value of CBPM2 includes the influence of beam jitter and beam trajectory tilt. And the contribution of the beam trajectory tilt can be separated by quadrature demodulation, as shown in Fig. 15(d). Furthermore, the equivalent beam position offsets after removing the trajectory tilt are shown

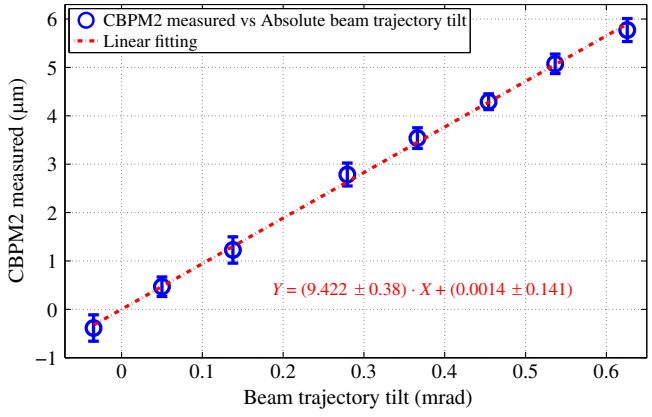

FIG. 16. The relationship between the CBPM2 demodulated and the absolute trajectory tilt converted by the CBPM1 and CBPM3.

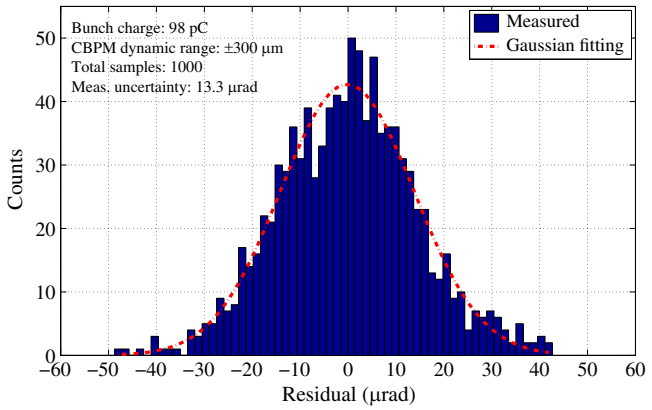

FIG. 17. Evaluation result of the beam trajectory tilt resolution based on the method of single cavity BPM.

in Fig. 15(c). By comparing the red samples, the position offset is close to zero, which reflects the practicability of the *in situ* demodulation method.

Also, the data of 3 cavity BPMs obtained by changing the corrector current from −1.2 to 2 A in the experiment were used, and about 600 sets data of CBPM2 by each current were demonstrated to get the beam trajectory tilt. Meanwhile, the linear relation between the absolute value of the trajectory tilt calculated by the CBPM1 and CBPM3 is shown in Fig. 16, which is consistent with the results of the Fig. 13 within the error range, and the reliability of the method of demodulation is also checked.

C. Performance evaluation

The resolution of *in situ* measurement of beam trajectory tilt using single cavity BPM was also evaluated based on the analysis and built of the beam test bench in the SXFEL. In the experiment, the corrector current was fixed at 1.2 A, and 1000 sets of data were accumulated for three cavity BPMs. The quadrature demodulation method was used to calculate the beam trajectory tilt measured by CBPM2. By combining the calculated values of CBPM1 and CBPM3, the correlation analysis method was used to evaluate the resolution of the beam trajectory tilt. The experimental results are shown in Fig. 17, it can be seen that the measured resolution of the system can reach 13.3 μrad at a bunch charge about 100 pC and the dynamic range of the system was controlled within ±300 μm, which also verifies the feasibility of this method.

V. CONCLUSION

Cavity BPMs are widely used in FEL facilities to achieve accurate measurement of multiparameters of electron beam, and it is a key equipment to ensure high-performance operation of the facility. However, the beam trajectory tilt often appears during operation, which can seriously affect the FEL radiation performance. Therefore, an *in situ* measurement method for beam position and trajectory tilt is needed to monitor the electron beam, especially in the compact undulation section. Based on this requirement, this paper proposes an *in situ* measurement method of beam trajectory tilt based on single cavity BPM, and the theoretical analysis and data processing method are completed. The beam test bench has also been built for verification and resolution evaluation. The experimental results are consistent with the theoretical analysis results, which verifies the feasibility of the method. Currently, this method is being implemented in the SXFEL facility to realize real-time monitoring of the status of electron beam.

VI. OUTLOOK

Based on the analysis presented in the paper, it can be inferred that the signal amplitude of trajectory tilt is directly proportional to the square of the cavity length. Therefore, increasing the cavity length appropriately is a key direction to enhance the resolution of trajectory tilt measurement, leading to increased signal amplitude and improved measurement resolution. Additionally, for achieving higher precision measurement, the use of multiple discrete BPMs for correlation analysis and the implementation of machine learning algorithms to eliminate common mode noise are effective measures to further enhance the accuracy and reliability of trajectory tilt measurement. Future research can focus on exploring these directions to improve the resolution and accuracy of trajectory tilt measurement, thereby supporting the high-performance operation of FEL facilities more effectively.

ACKNOWLEDGMENTS

This work was supported by the National Key Research and Development Program of China under Grant No. 2016YFA0401903 and the Young and Middle-Aged Leading Scientists, Engineers and Innovators through the Ten Thousand Talent Program.

[1] E. J. Jaeschke, S. Khan, J. R. Schneider, and J. B. Hastings, *Synchrotron Light Sources and Free-Electron Lasers: Accelerator Physics, Instrumentation and Science Applications* (Springer, New York, 2016).

[2] U. Bergmann, J. Corlett, S. Dierker, R. Falcone, J. Galayda, M. Gibson, J. Hastings, B. Hettel, J. Hill, Z. Hussain, C.-C. Kao, a. J. Kirz, G. Long, B. McCurdy, T. Raubenheimer, F. Sannibale, J. Seeman, Z. X. Shen, G. Shenoy, B. Schoenlein, Q. Shen, S. /Argonne /Brookhaven /LBL, and Berkeley /SLAC, Science and technology of future light sources: A white paper, 10.2172/947109 (2009).

[3] C. Feng and H.-X. Deng, Review of fully coherent free-electron lasers, Nucl. Sci. Tech. **29**, 160 (2018).

[4] T. Tanaka, H. Kitamura, and T. Shintake, Consideration on the BPM alignment tolerance in x-ray FELs, Nucl. Instrum. Methods Phys. Res., Sect. A **528**, 172 (2004), proceedings

of the 25th International Free Electron Laser Conference, and the 10th FEL Users Workshop.

[5] L. Zeng, C. Feng, D. Gu, J. Li, and Z. Zhao, The beam-based alignment for soft x-ray free-electron lasers via genetic algorithm, Nucl. Instrum. Methods Phys. Res., Sect. A **905**, 104 (2018).

[6] H. Maesaka, H. Ego, S. Inoue, S. Matsubara, T. Ohshima, T. Shintake, and Y. Otake, Sub-micron resolution rf cavity beam position monitor system at the SACLA XFEL facility, Nucl. Instrum. Methods Phys. Res., Sect. A **696**, 66 (2012).

[7] V. Sargsyan, Comparison of stripline and cavity beam position monitors, TESLA Report No. 2004-03, 2004, https://citeseerx.ist.psu.edu/doc/10.1.1.9.7483.

[8] Z. Li, R. Johnson, S. R. Smith, /SLAC, T. Naito, T. /KEK, and J. Rifkin, Cavity BPM with dipole-mode-selective coupler, in *Particle Accelerator Conference (PAC 03), Portland, Oregon, 2003* (Stanford Linear Accelerator Center, 2006), https://www.osti.gov/biblio/884883.

[9] G. Mazaheri, T. Slaton, and T. Shintake, Development of nanometer resolution C-band radio frequency beam position monitors in the final focus test-beam, AIP Conf. Proc. **451**, 394 (1998).

[10] S. Walston, S. Boogert, C. Chung, P. Fitsos, J. Frisch, J. Gronberg, H. Hayano, Y. Honda, Y. Kolomensky, A. Lyapin, S. Malton, J. May, D. McCormick, R. Meller, D. Miller, T. Orimoto, M. Ross, M. Slater, S. Smith, T. Smith, N. Terunuma, M. Thomson, J. Urakawa, V. Vogel, D. Ward, and G. White, Performance of a high resolution cavity beam position monitor system, Nucl. Instrum. Methods Phys. Res., Sect. A **578**, 1 (2007).

[11] M. Stadler, R. Baldinger, R. Ditter, B. Keil, R. Kramert, G. Marinkovic, and M. Roggli, Beam test results of undulator cavity BPM electronics for the European XFEL, in *Proceeding of International Beam Instrumentation Conference (IBIC'12)* (JACoW, Geneva, 2012), pp. 404–408.

[12] R. Lill, W. Norum, L. Morrison, N. Sereno, G. Waldschmidt, D. Walters, S. Smith, and T. Straumann, Design and performance of the LCLS cavity BPM system, in *Proceedings of the 2007 IEEE Particle Accelerator Conference (PAC)* (JACoW, Albuquerque, NM, 2007), pp. 4366–4368.

[13] S. Smith, S. Hoobler, R. Johnson, T. Straumann, A. Young, R. Lill, L. Morrison, W. Norum, N. Sereno, G. Waldschmidt, and D. Walters, Commissioning and performance of LCLS cavity BPMs, in *2009 Particle Accelerator Conference (PAC)* (JACoW, Vancouver, BC, 2009), pp. 754–756.

[14] H. Wiedemann, Beam-cavity interaction, in *Particle Accelerator Physics* (Springer International Publishing, Cham, 2015), pp. 641–665.

[15] D. H. Whittum and Y. Kolomensky, Analysis of an asymmetric resonant cavity as a beam monitor, Rev. Sci. Instrum. **70**, 2300 (1999).

[16] R. Lorenz, Cavity beam position monitors, AIP Conf. Proc. **451**, 53 (1998).

[17] D. Lipka, Cavity BPM designs, related electronics and measured performances, in *Proceedings of the 9th European Workshop on Beam Diagnostics and Instrumentation for Particle Accelerators Conference(DIPAC'09), Besel, Switzerland, 2009* (JACoW, Geneva, 2009), pp. 280–284.

[18] J. Chen, Y. Leng, S. Cao, L. Lai, R. Yuan, R. Jiang, and X. Yang, Optimized design method study for cavity bpm system, Nucl. Instrum. Methods Phys. Res., Sect. A **1044**, 167509 (2022).

[19] S. Hartman, T. Shintake, and N. Akasaka, Nanometer resolution BPM using damped slot resonator, in *Proceedings Particle Accelerator Conference* (JACoW, Texas, 1995), Vol. 4, pp. 2655–2657.

[20] Y. Inoue, H. Hayano, Y. Honda, T. Takatomi, T. Tauchi, J. Urakawa, S. Komamiya, T. Nakamura, T. Sanuki, E.-S. Kim, S.-H. Shin, and V. Vogel, Development of a high-resolution cavity-beam position monitor, Phys. Rev. ST Accel. Beams **11**, 062801 (2008).

[21] J. Chen, Y.-B. Leng, L.-Y. Yu, L.-W. Lai, and R.-X. Yuan, Study of the crosstalk evaluation for cavity BPM, Nucl. Sci. Tech. **29**, 83 (2018).

[22] D. Wang and W. Wan, X-ray FEL facilities at Shanghai, in *Proceedings of International Computational Accelerator Physics Conference (ICAP'18), Key West, FL, USA, 2018* (JACoW, Geneva, Switzerland, 2019) presented at ICAP2018 in Key West, FL, USA.

[23] J. Chen, S. Cao, L. Lai, Y. Leng, and R. Yuan, Development of the prototype of the cavity BPM system for SHINE, in *Proceedings of the IPAC'21* (JACoW Publishing, Geneva, Switzerland, 2021), pp. 4552–4555, 10.18429/JACoW-IPAC2021-FRXC06.

[24] S. Cao, R. Jiang, Y. Leng, and R. Yuan, Design and test of CBPM prototypes for SHINE, in *Proceedings of the IBIC'20* (JACoW Publishing, Geneva, Switzerland, 2020), pp. 124–127, 10.18429/JACoW-IBIC2020-WEPP13.

[25] L. Lai and Y. Leng, High-speed beam signal processor for SHINE, in *Proceedings of the IBIC'19* (JACoW Publishing, Geneva, Switzerland, 2019), pp. 283–284, 10.18429/JACoW-IBIC2019-TUPP004.

[26] J. Chen, S. Cao, Y. Leng, T. Wu, and Y. Zhou, Study of the optimal amplitude extraction algorithm for cavity BPM, Nucl. Instrum. Methods Phys. Res., Sect. A **1012**, 165627 (2021).

[27] J. Chen, Y.-B. Leng, L.-Y. Yu, L.-W. Lai, and R.-X. Yuan, Optimization of the cavity beam-position monitor system for the shanghai soft x-ray free-electron laser user facility, Nucl. Sci. Tech. **33**, 124 (2022).

[28] Z. Zhao, Status of SXFEL test and user facilities, in *Proceedings of the Free Electron Laser Conference (FEL'19)* (JACoW, Geneva, Switzerland, 2019).

[29] C. Feng, H. Deng, M. Zhang, X. Wang, S. Chen, T. Liu, K. Zhou, D. Gu, Z. Wang, Z. Jiang, X. Li, B. Wang, W. Zhang, T. Lan, L. Feng, B. Liu, Q. Gu, Y. Leng, L. Yin, D. Wang, Z. Zhao, G. Wang, and D. Xiang, Coherent extreme ultraviolet free-electron laser with echo-enabled harmonic generation, Phys. Rev. Accel. Beams **22**, 050703 (2019).